High Power Laser Science and Engineering, (2023), Vol. 11, e53, 6 pages.
doi:10.1017/hpl.2023.42

HIGH POWER LASER SCIENCE AND ENGINEERING

RESEARCH ARTICLE

High-power mid-infrared femtosecond master oscillator power amplifier Er:ZBLAN fiber laser system

Linpeng Yu[1,†], Jinhui Liang[1,†], Qinghui Zeng[1], Jiacheng Wang[1], Xing Luo[1], Jinzhang Wang[1], Peiguang Yan[1], Fanlong Dong[1], Xing Liu[2], Qitao Lü[3], Chunyu Guo[1], and Shuangchen Ruan[1,2]

[1] *Shenzhen Key Laboratory of Laser Engineering, Guangdong Provincial Key Laboratory of Micro/Nano Optomechatronics Engineering, Key Laboratory of Optoelectronic Devices and Systems of Ministry of Education and Guangdong Province, State Key Laboratory of Radio Frequency Heterogeneous Integration, College of Physics and Optoelectronic Engineering, Shenzhen University, Shenzhen, China*

[2] *Key Laboratory of Advanced Optical Precision Manufacturing Technology of Guangdong Higher Education Institutes, Shenzhen Technology University, Shenzhen, China*

[3] *Han's Laser Technology Industry Group Co., Ltd., Shenzhen, China*

(Received 4 March 2023; revised 28 April 2023; accepted 11 May 2023)

Abstract

High-power femtosecond mid-infrared (MIR) lasers are of vast importance to both fundamental research and applications. We report a high-power femtosecond master oscillator power amplifier laser system consisting of a single-mode Er:ZBLAN fiber mode-locked oscillator and pre-amplifier followed by a large-mode-area Er:ZBLAN fiber main amplifier. The main amplifier is actively cooled and bidirectionally pumped at 976 nm, generating a slope efficiency of 26.9%. Pulses of 8.12 W, 148 fs at 2.8 μm with a repetition rate of 69.65 MHz are achieved. To the best of our knowledge, this is the highest average power ever achieved from a femtosecond MIR laser source. Such a compact ultrafast laser system is promising for a wide range of applications, such as medical surgery and material processing.

Keywords: femtosecond fiber laser; fluoride fiber amplifier; master oscillator power amplifier; mid-infrared

1. Introduction

Mid-infrared (MIR) laser sources operating in the spectral range of 2–5 μm are of great significance owing to their widespread applications in molecular spectroscopy, medical surgery, material processing, strong-field physics and defense and security[1–6]. In the last decade, fluoride fiber lasers have attracted increasing attention as a simple and economic way to directly generate MIR laser radiation. Compared with traditional silica fibers that transmit up to 2.2 μm, fluoride fibers have a much larger transmission-window long-wavelength edge of 5 μm. Meanwhile, fluoride fibers can be doped with various rare earth ions, such as dysprosium[7], holmium[8] and erbium[9–12], enabling the generation of coherent continuous-wave (CW) or pulsed light at 2.8 μm or even longer wavelengths. Among all rare-earth-doped fluoride fibers, erbium-doped fluoride fibers (typically Er:ZBLAN fibers) are currently the most successful gain medium for fiber laser operation in the MIR region due to their simple pumping scheme and high gain efficiency around 2.8 μm[9,10]. To date, based on heavily doped Er:ZBLAN fibers, the highest average power for a CW laser can reach 41.6 W[11], while it is 70 W for a quasi-CW laser[12].

More recently, motivated by numerous potential applications, there has been a continuously growing interest in developing high-power femtosecond lasers[13–18]. Generally, the output power of mode-locked Er:ZBLAN fiber oscillators is limited to hundreds of milliwatts[13], while further power enhancement requires external amplification. The first reported watt-level femtosecond Er:ZBLAN fiber laser system was demonstrated by Duval *et al.*[14]. Their laser system consisted of a nonlinear polarization rotation (NPR) mode-locked oscillator and one-stage amplifier, constituting a master oscillator power amplifier (MOPA) configuration.

Correspondence to: Chunyu Guo, College of Physics and Optoelectronic Engineering, Shenzhen University, Shenzhen 518060, China. E-mail: cyguo@szu.edu.cn

[†]These authors contributed equally to this work.

Later, Cui *et al.*[15] realized a sub-100-fs pulse with an average power of 2.4 W at 2.85 μm through simultaneous pulse amplification and soliton self-compression in an Er:ZBLAN fiber amplifier. Last year, we reported on the generation of 4.13 W, 59 fs pulses at 2.8 μm from a nonlinear Er:ZBLAN fiber amplifier through optimization of the input polarization and pumping scheme[16]. However, upon a further increase in the pump power, detrimental nonlinear effects, such as the Raman effect[14,18–20], will become significant, hindering the output power scaling. Moreover, powerful pumping will result in overheating of the fiber end, which will bring additional challenges to the thermal management of the laser system. Therefore, continuous efforts are still needed to improve the performance of high-power MIR femtosecond laser systems.

Large fiber nonlinearity due to the small core size of conventional single-mode Er:ZBLAN fibers is the crucial obstacle to boosting the output power. A straightforward way to weaken the fiber nonlinearity is to utilize large-mode-area (LMA) Er:ZBLAN fibers, which can reduce the accumulation of nonlinear phase shift and thereby avoid the temporal distortion of femtosecond pulses during the amplification process. In addition, a larger core size favors a higher damage threshold of the fiber. Thus, by cascading an LMA Er:ZBLAN fiber amplifier to a single-mode Er:ZBLAN fiber pre-amplifier, a higher output power can be expected without degrading the temporal pulse quality. Such an LMA-fiber-based multi-stage MOPA configuration has been recently demonstrated in the long-pulse (ns-range) regime[21,22], whereas few studies have been reported in high-power femtosecond laser systems.

In this paper, we report a high-power femtosecond MOPA laser system consisting of a single-mode Er:ZBLAN fiber mode-locked oscillator and a pre-amplifier followed by an LMA Er:ZBLAN fiber main amplifier. The system delivers 8.12 W, 148 fs pulses at 2.8 μm with a repetition rate of 69.65 MHz and M^2 factors of less than or equal to 1.3. Employment of the LMA Er:ZBLAN fiber effectively reduces the fiber nonlinearity and allows the high-power operation of the main amplifier. To the best of our knowledge, this is the highest average power ever achieved from a femtosecond MIR laser source. The high average power and short pulse duration make the system a promising tool for a wide range of applications.

2. Experimental setup

The schematic of the experimental setup is shown in Figure 1. The system consists of a femtosecond NPR mode-locked oscillator, a single-mode Er:ZBLAN fiber pre-amplifier and an LMA Er:ZBLAN fiber main amplifier. The oscillator and pre-amplifier are similar to that described in Ref. [16]. The oscillator delivers 257 fs, 2.8 nJ seed pulses at 2.8 μm with a repetition rate of 69.65 MHz. In the pre-amplifier, a 3.1-m-length 7% (molar fraction) single-mode Er:ZBLAN fiber (Le Verre Fluoré) is used as the gain fiber, which has a core diameter of 15 μm (NA = 0.12) surrounded by a truncated 260-μm diameter inner cladding (NA = 0.45). The gain fiber is backward-pumped by a high-power 976-nm laser diode (LD) with a pigtail output fiber of 105-μm core diameter (NA = 0.22). Under a pump power of 10 W, the seed pulses are amplified to an average power of 2.39 W by the pre-amplifier, corresponding to an estimated pulse energy of 34.3 nJ.

The pre-amplified signal light then passes through a polarization-dependent isolator to block backward reflections from the main amplifier. A quarter-wave plate and a half-wave plate are utilized to adjust the polarization of the signal light. Before being launched into the main amplifier, the available power of the linearly polarized signal light is only 1.15 W due to the large propagation loss. In the main amplifier, a 4-m-length 6% (molar fraction) double-clad LMA Er:ZBLAN fiber (Fiberlabs) is employed as the gain fiber, which has a core diameter of 30 μm (NA = 0.12) and an inner cladding diameter of 300 μm (NA = 0.51).

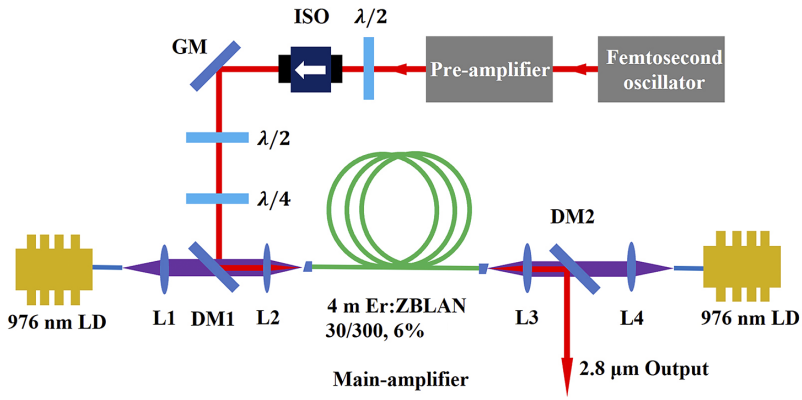

Figure 1. Schematic of the laser system. ISO, isolator; GM, gold mirror; LD, laser diode; λ/2, half-wave plate; λ/4, quarter-wave plate; DM, dichroic mirror; L, lens.

Such a large core size ensures low fiber nonlinearity and high energy storage capacity of the main amplifier. On the downside, the large core size yields a V number of 4.04 at 2.8 μm and supports six degenerate waveguide modes, which will degrade the beam quality. To suppress the high-order transverse modes, the LMA Er:ZBLAN fiber is coiled with a diameter of 14 cm. In addition, the *XYZ* position of the input fiber end is carefully adjusted to favor the excitation of the fundamental mode, thus improving the output beam quality. This process results in a low signal power of 0.4 W after the rear fiber end, yielding an estimated coupling efficiency of 35%. The soliton order of the incident pulse to the main amplifier is calculated to be 0.42. To prevent fiber tip degradation and optical damage, both two fiber ends are protected with approximately 400 μm long AlF_3 endcaps. The endcaps, with a 450-μm core size (Le Verre Fluoré), are cleaved at an angle of 8° to avoid parasitic lasing. To reduce the maximum temperature at the rear end of the gain fiber, a dual-end pumping scheme is employed, so that both fiber ends can share the pump heat load. Moreover, both fiber ends are mounted onto water-cooled metal fixtures, while the protruding bare-fiber portions are blown with cold nitrogen gas under high-power operation for thermal management. The nitrogen atmosphere can also prevent moisture in the air from inducing optical damage at the fiber ends[12,23]. The other parts of the gain fiber are passively cooled by placing them on an aluminum plate covered with thermally conductive silicone grease. The pump light is coupled into the gain fiber by employing plano-convex BK7 lenses (L1, L4, $f = 10$ mm) and aspheric CaF_2 lenses (L2, L3, $f = 20$ mm).

3. Results and discussion

3.1. Er:ZBLAN fiber pre-amplifier

The output spectrum of the Er:ZBLAN fiber pre-amplifier under a pump power of 10 W is measured by an optical spectrum analyzer (Yokogawa, AQ6376), and is shown in Figure 2(a). It is observed that the signal pulses experience a significant symmetric spectral broadening due to the self-phase modulation (SPM) effect, covering the wavelength range from 2648 to 2943 nm at the –30 dB level. The pulse duration is characterized using a commercial intensity auto-correlator (Femtochrome, FR-103XL). Figure 2(b) displays the measured autocorrelation trace. Assuming a hyperbolic-secant pulse shape, the pulse duration is calculated to be 97 fs. The radio frequency (RF) spectrum measured by an RF spectrum analyzer (Rohde & Schwarz FSWP) is presented in Figure 2(c), which exhibits a high signal-to-noise ratio (SNR) of 75 dB at the fundamental frequency. Figure 2(d) shows the pulse trains monitored by an MIR photodetector (VIGO System, PCI-9) in the 200-ns and 20-ms time scales. No obvious modulation is observed, revealing a high temporal stability.

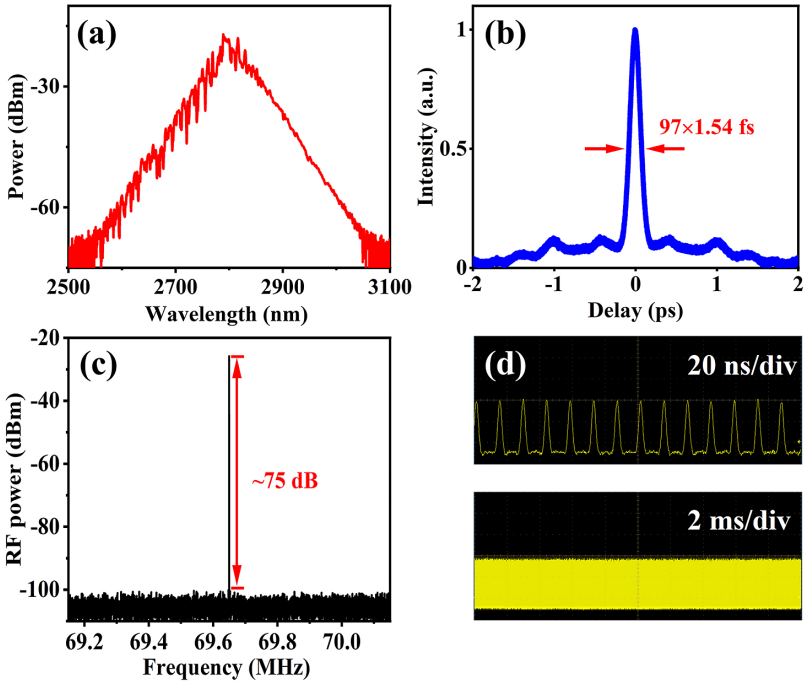

Figure 2. Measured output characteristics of the pre-amplifier under a pump power of 10 W. (a) Output spectrum. (b) Autocorrelation trace. (c) RF spectrum with a resolution bandwidth of 10 Hz. (d) Pulse trains in the nanosecond and millisecond time scales.

3.2. Er:ZBLAN fiber main amplifier

Figure 3 depicts the average output power as a function of the total launched pump power in the main amplifier. It is seen that the output power increases linearly with the pump power. A slope efficiency of 26.9% is obtained by linear fitting. No saturation of the laser curve is observed, indicating that the output power of the laser system has the potential to be further scaled up. The highest output power of 8.12 W is obtained when the total launched pump power reaches 28.8 W, corresponding to an estimated pulse energy of 116.6 nJ. The temperature of the rear fiber end is measured to be approximately 60°C by a thermal camera under this launched pump power. Further increasing of the pump power would increase the risk of fiber tip damage due to overheating. The output pulse durations attained at different pump power levels are also presented in Figure 3. Under a relatively low pump power, the pulse duration is stretched to sub-picoseconds because the SPM effect cannot balance the large anomalous dispersion provided by the LMA Er:ZBLAN fiber. With increasing of the pump power, the signal pulses are not only amplified but also compressed, which is known as the soliton self-compression effect[15,16]. The evolutions of the output spectra and corresponding autocorrelation traces are shown in Figures 4(a) and 4(b), respectively. Compared with the input spectrum shown in Figure 2(a), the output spectrum in the top panel of Figure 4(a) is mainly reshaped by the gain narrowing effect of the main amplifier. As the output power increases, the nonlinear spectral broadening is gradually enhanced and finally dominates the spectral reshaping process, as shown

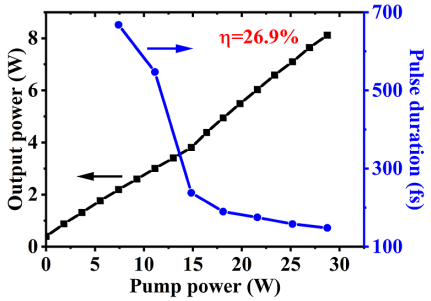

Figure 3. Average output power and pulse duration of the main amplifier versus pump power.

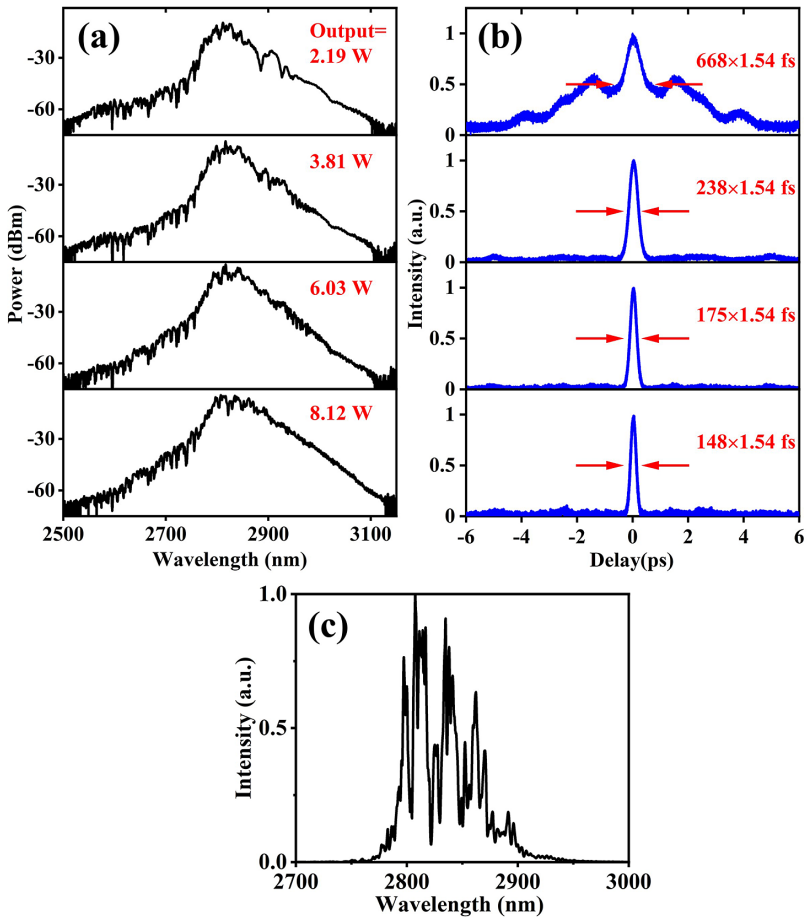

Figure 4. (a) Output spectra and (b) corresponding autocorrelation traces of the main amplifier at different average output power levels. (c) Linear output spectrum of the main amplifier at an average output power of 8.12 W.

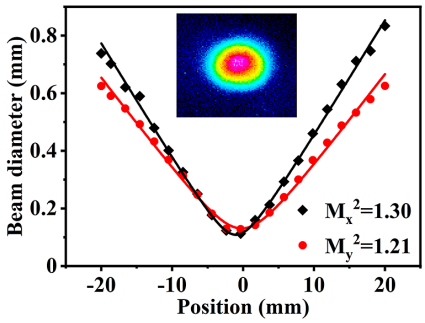

Figure 5. Beam quality measurement of the main amplifier at an average output power of 6.28 W. Inset: the corresponding collimated beam profile.

in the bottom panel of Figure 4(a). At the highest average output power of 8.12 W, the signal pulses are compressed to 148 fs, corresponding to a peak power of 787.7 kW. The linear output spectrum is presented in Figure 4(c), corresponding to a Fourier-transform-limited pulse duration of 145 fs. No nonlinearity induced soliton fission occurs during the amplification process. It can be inferred that the accumulation of nonlinear phase shift is effectively reduced as expected, thus allowing the high-power operation of the main amplifier.

As an important parameter of LMA fiber laser sources, the output beam quality is characterized. Figure 5 depicts the measurement results of the M^2 factor at an average output power of 6.28 W, in which the inset shows the corresponding collimated beam profile. The beam profile exhibits a slightly elliptical shape, which should be caused by the high-order transverse modes induced by the AlF_3 endcap of the rear fiber end. The M^2 values are measured to be 1.30 for the x-axis and 1.21 for the y-axis, yielding an average M^2 value of 1.26. Such a beam quality is acceptable for our high-power femtosecond laser system. To reduce the M^2 values of the output beam and obtain a nearly diffraction-limited beam quality, the fusion-spliced endcap should be optimized. Moreover, LMA gain fibers with a small NA that only support the operation of the fundamental mode are in high demand.

The long-term power stability of the laser system is also evaluated by monitoring the average output power over 1 hour (acquisition rate = 1 Hz). As illustrated in Figure 6(a), a normalized root-mean-square (RMS) deviation of 1.3% is obtained at an average output power of 6.28 W. It is suspected that the slight power fluctuation results from the disturbance of nitrogen purging. The corresponding pulse train measured in a 20-ms time scale is presented in the inset of Figure 6(a), which shows no obvious modulation. Moreover, the RF spectrum is also measured and is depicted in Figure 6(b). A reduced SNR value of 51 dB at the fundamental frequency is obtained.

4. Conclusion

In summary, a high-power MIR femtosecond MOPA fluoride fiber laser system is demonstrated, which is composed of a single-mode Er:ZBLAN fiber mode-locked oscillator and a pre-amplifier followed by an LMA Er:ZBLAN fiber main amplifier. For thermal management, the main amplifier is actively cooled and bidirectionally pumped at 976 nm. Incorporation of the LMA Er:ZBLAN fiber effectively reduces the accumulation of nonlinear phase shift, enabling the high-power operation of the main amplifier before pulse splitting. Based on this laser system, 8.12 W, 148 fs pulses at 2.8 μm with a repetition rate of 69.65 MHz and M^2 factors of less than or equal to 1.3 are generated, which are the highest-average-power femtosecond pulses ever achieved from an MIR laser source to date. Such a compact high-power ultrafast laser system is very attractive for applications in medical surgery and material processing. Note that the achieved highest average power is limited by the high thermal load on the rear fiber end of the main amplifier. For scaling to a higher average power, it is suggested to optimize the core/clad ratio and doping concentration of the gain fiber, or use pump LDs with center wavelengths deviating from the peak absorption wavelength at 976 nm, thereby reducing the heat load along the fiber[21]. Moreover, an additional amplification stage involving a larger-mode-area Er:ZBLAN fiber

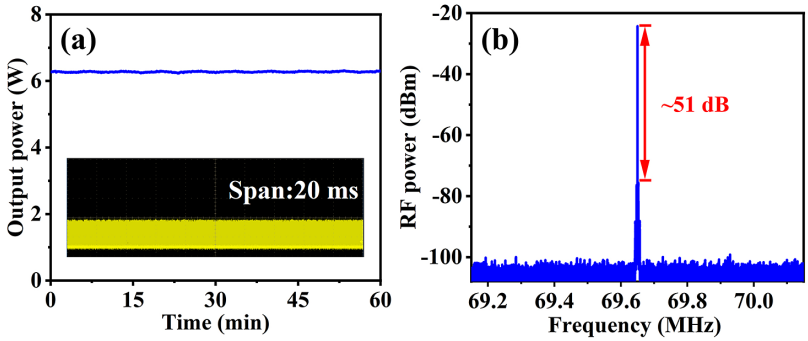

Figure 6. (a) Measured long-term stability of the main amplifier for 1 hour at an average output power of 6.28 W. Inset: the corresponding pulse train measured in a 20-ms time scale. (b) RF spectrum with a resolution bandwidth of 10 Hz.

after the main amplifier would contribute to the generation of femtosecond pulses with tens of watts of average power.

Acknowledgements

This work was supported by the National Natural Science Foundation of China (61975136, 61935014, 62105222, 61775146, 61905151), the Basic and Applied Basic Research Foundation of Guangdong Province (2019A1515010699), the Shenzhen Science and Technology Innovation Program (CJGJZD20200617103003009, JCYJ20210324094400001, GJHZ20210705141801006) and the Beijing Natural Science Foundation (JQ21019).

References

1. S. D. Jackson, Nat. Photonics **6**, 423 (2012).
2. A. Schliesser, N. Picqué, and T. W. Hänsch, Nat. Photonics **6**, 440 (2012).
3. E. Sorokin, I. T. Sorokina, J. Mandon, G. Guelachvili, and N. Picqué, Opt. Express **15**, 16540 (2007).
4. A. H. Nejadmalayeri and P. R. Herman, Opt. Lett. **30**, 964 (2005).
5. G. Vampa, T. J. Hammond, M. Taucer, X. Ding, X. Ropagnol, T. Ozaki, S. Delprat, M. Chaker, N. Thiré, B. E. Schmidt, F. Légaré, D. D. Klug, A. Y. Naumov, D. M. Villeneuve, A. Staudte, and P. B. Corkum, Nat. Photonics **12**, 465 (2018).
6. H. H. P. Th. Bekman, J. C. van den Heuvel, F. J. M. van Putten, and R. Schleijpen, Proc. SPIE **5615**, 27 (2004).
7. V. Fortin, F. Jobin, M. Larose, M. Bernier, and R. Vallée, Opt. Lett. **44**, 491 (2019).
8. S. Antipov, D. D. Hudson, A. Fuerbach, and S. D. Jackson, Optica **3**, 1373 (2016).
9. D. Faucher, M. Bernier, G. Androz, N. Caron, and R. Vallée, Opt. Lett. **36**, 1104 (2011).
10. Y. O. Aydin, V. Fortin, F. Maes, F. Jobin, S. D. Jackson, R. Vallée, and M. Bernier, Optica **4**, 235 (2017).
11. Y. O. Aydin, V. Fortin, R. Vallée, and M. Bernier, Opt. Lett. **43**, 4542 (2018).
12. G. A. Newburgh and M. Dubinskii, Laser Phys. Lett. **18**, 095102 (2021).
13. F. Jobin, P. Paradis, Y. O. Aydin, T. Boilard, V. Fortin, J. Gauthier, M. Lemieux-Tanguay, S. Magnan-Saucier, L. Michaud, S. Mondor, L. Pleau, L. Talbot, M. Bernier, and R. Vallée, Opt. Express **30**, 8615 (2022).
14. S. Duval, J. Gauthier, L. Robichaud, P. Paradis, M. Olivier, V. Fortin, M. Bernier, M. Piché, and R. Vallée, Opt. Lett. **41**, 5294 (2016).
15. Y. Cui, M. Chen, W. Du, Y. Bai, and A. Galvanauskas, Opt. Express **29**, 42924 (2021).
16. L. Yu, J. Liang, S. Huang, J. Wang, J. Wang, X. Luo, P. Yan, F. Dong, X. Liu, Q. Lue, C. Guo, and S. Ruan, Opt. Lett. **47**, 2562 (2022).
17. J. Huang, M. Pang, X. Jiang, F. Köttig, D. Schade, W. He, M. Butryn, and P. St. J. Russell, Optica **7**, 574 (2020).
18. L. Yu, J. Liang, S. Huang, J. Wang, J. Wang, X. Luo, P. Yan, F. Dong, X. Liu, Q. Lue, C. Guo, and S. Ruan, Photonics Res. **10**, 2140 (2022).
19. M. Wang, H. Zhang, R. Wei, Z. Zhu, S. Ruan, P. Yan, J. Wang, T. Hasan, and Z. Sun, Opt. Lett. **43**, 4619 (2018).
20. I. Tiliouine, H. Delahaye, G. Granger, Y. Leventoux, C. E. Jimenez, V. Couderc, and S. Février, Opt. Lett. **46**, 5890 (2021).
21. Y. O. Aydin, S. Magnan-Saucier, D. Zhang, V. Fortin, D. Kraemer, R. Vallée, and M. Bernier, Opt. Lett. **46**, 4506 (2021).
22. W. Du, Y. Bai, Y. Cui, M. Chen, and A. Galvanauskas, Opt. Express **30**, 46170 (2022).
23. S. Tokita, M. Murakami, S. Shimizu, M. Hashida, and S. Sakabe, Opt. Lett. **36**, 2812 (2011).